Continuum description of damage in ceramic-matrix composites

A. BURR *, F. HILD *[1] and F. A. LECKIE **

ABSTRACT. – A constitutive law is proposed for Ceramic-Matrix Composites which models matrix-cracking, interface debonding and sliding, fiber-breakage, and fiber pull-out. These different mechanisms induce loss of stiffness, inelastic strains, hysteresis loops, and crack closure. The features are analyzed within the framework of Continuum Damage Mechanics by the introduction of physical internal variables identified previously in material science investigations. The procedure is applied to a SiC/SiC [0/90] laminate composite using the results of pure tension tests of two laminate orientations. Each test involves a series of loading and unloading sequences. In order to verify the material description the behavior of an Iosipescu shear test is predicted using a Finite Element calculation and the results are compared with experiment.

Nomenclature

a	crack size
α	inelastic strain
$\underline{\underline{\alpha}}$	inelastic strain tensor
α_i	inelastic strain component in the i-direction (i = 11 or 22)
α_{11}, α_{22}, α_{12}	components of the inelastic strain tensor $\underline{\underline{\alpha}}$ in 1-2 frame
d	damage variable due to debonding and slip
$\underline{\underline{d}}$	debonding and sliding damage tensor
d_{11}, d_{22}, d_{12}	components of the debonding and sliding damage tensor $\underline{\underline{d}}$ in 1-2 frame
D, D_m, D_{my}, D_{my}^{00}, D_{my}^{90}	damage variables modeling matrix-cracking
$\overline{D}$, $\overline{D}^{00}$, $\overline{D}^{45}$	macroscopic damage variables
D_f, D_{f1}, D_{f1}^{00}, D_{f1}^{90}	damage variables modeling fiber-breakage
D_i	set of damage variables
D_{sat}, Y_{mth}, Y_{m0}, m_m	parameters of the evolution law of matrix-cracking damage
Δ_S	crack opening displacement due to slip
$\delta\bar{\varepsilon}$, $\delta\bar{\varepsilon}^{00}$, $\delta\bar{\varepsilon}^{45}$	maximum hysteresis loop widths
E, E_1, E_2, E_m, E_f	Young's moduli
E^{00}	Young's modulus of the 0-degree layer in the fiber direction
E^{90}	Young's modulus of the 90-degree layer in the fiber direction
$\overline{E}$	equivalent Young's modulus
$\tilde{E}$	Young's modulus of a damaged material

* Laboratoire de Mécanique et Technologie, ENS de Cachan/CNRS/Université Paris-VI, 61, avenue du Président Wilson, 94235 Cachan Cedex, France.

** Department of Mechanical and Environmental Engineering, College of Engineering, University of California, Santa Barbara CA 93106-5070, U.S.A.

[1] To whom correspondence should be addressed

$\underline{\underline{\underline{\underline{E}}}}\left(D_{my},\, D_{f1}^{00},\, D_{f1}^{90}\right)$	fourth order elastic tensor on the composite level of a woven composite
$\underline{\underline{\underline{\underline{E}}}}\left(D_{my}^{00},\, D_{my}^{90},\, D_{f1}^{00},\, D_{f1}^{90}\right)$	fourth order elastic tensor on the composite level
$\underline{\underline{\underline{\underline{E}}}}^{L}\left(D_{my},\, D_{f1}\right)$	fourth order elastic tensor on the layer level
$\underline{\underline{\underline{\underline{E}}}}^{00}\left(D_{my}^{00},\, D_{f1}^{00}\right)$	fourth order elastic tensor of the 0-degree layer
$\underline{\underline{\underline{\underline{E}}}}^{90}\left(D_{my}^{90},\, D_{f1}^{90}\right)$	fourth order elastic tensor of the 90-degree layer
$\overline{\varepsilon}$	macroscopic strain
$\underline{\underline{\varepsilon}}$	overall strain tensor
$\varepsilon_{11},\, \varepsilon_{22},\, \varepsilon_{12}$	component of the strain tensor $\underline{\underline{\varepsilon}}$ in 1-2 frame
$\underline{\underline{\varepsilon}}_f^i$	strain tensor in the fiber aligned along the i-direction
$\varepsilon_{f11},\, \varepsilon_{f22},\, \varepsilon_{f12}$	component of the strain tensor $\underline{\underline{\varepsilon}}_f$ of the fiber in 1-2 frame
$\overline{\varepsilon}_{in}$	inelastic strain upon complete unloading ($\overline{\sigma} = 0$)
$\overline{\varepsilon}_{in}^{00},\, \overline{\varepsilon}_{in}^{45}$	macroscopic inelastic strain upon complete unloading
$\underline{\underline{\varepsilon}}^{L},\, \underline{\underline{\varepsilon}}^{00},\, \underline{\underline{\varepsilon}}^{90}$	strain tensor on a layer level
$\varepsilon_{mxx},\, \varepsilon_{myy},\, \varepsilon_{mxy}$	components of the strain tensor $\underline{\underline{\varepsilon}}_m$ of the matrix in x-y frame
$\varepsilon_{m11},\, \varepsilon_{m22},\, \varepsilon_{m12}$	components of the strain tensor $\underline{\underline{\varepsilon}}_m$ of the matrix in 1-2 frame
$\overline{\varepsilon}_M,\, \overline{\varepsilon}_M^{00},\, \overline{\varepsilon}_M^{45}$	maximum applied strain
$f,\, f_f$	fiber volume fraction
f_m	matrix volume fraction
$f^{00},\, f^{90}$	volume fraction of the 0-degree and the 90-degree layer
F	set of associated forces
G	energy release rate
$\overline{G}$	equivalent shear modulus
$\tilde{G}_f$	shear modulus of the damaged fiber embedded in the matrix
$G_m,\, \tilde{G}_m$	shear modulus of the undamaged and damaged matrix
G^{00}	shear modulus of the 0-degree layer
G^{90}	shear modulus of the 90-degree layer
L	crack spacing
l_F	friction length (assumed to be equal to debond length l_d)
ν_m	Poisson's ratio of the matrix
R	fiber radius
S	set of state variables
ψ	Helmholtz free energy density (state potential)
ψ^D	elastic energy density on the composite level
ψ^e	elastic (or reversible) free energy density
ψ_f	elastic energy density of the fiber
ψ^s	stored free energy density
ψ^S	stored energy density due to debonding and sliding of a composite
ψ^L	elastic energy density on the layer level
ψ_m	elastic energy density of the matrix
ψ^{00}	free energy density of the layer at 0 degree
ψ^{90}	free energy density of the layer at 90 degrees
ρ_1	residual stress in the matrix
ρ_1^{00}	residual stress in the broken part of the 0-degree layer
σ	effective (or microscopic) stress
$\overline{\sigma}$	macroscopic stress
$\underline{\underline{\sigma}}$	overall stress tensor
$\sigma_{11},\, \sigma_{22},\, \sigma_{12}$	components of the stress tensor $\underline{\underline{\sigma}}$ in 1-2 frame
$\underline{\underline{\sigma}}_f$	stress tensor of the fiber
$\underline{\underline{\sigma}}_f^i$	stress tensor in the fiber aligned along the i-direction
σ_i	stress applied to the composite in the i-direction (i = 11 or 22)
$\underline{\underline{\sigma}}^{L},\, \underline{\underline{\sigma}}^{00},\, \underline{\underline{\sigma}}^{90}$	stress tensor on a layer level

$\underline{\underline{\sigma}}_m$	stress tensor of the matrix
$\overline{\sigma}_M$, $\overline{\sigma}_M^{00}$	maximum applied stress
σ_{th}, σ_0, τ_{th}, τ_0	parameters of the evolution law of the inelastic strains
τ_{eq}	equivalent shear stress
W	width
X	back-stress
$\underline{\underline{X}}$	back-stress tensor
X_{11}, X_{22}, X_{12}	components of the back-stress tensor $\underline{\underline{X}}$ in 1-2 frame
y	debonding and friction energy release rate density
$\underline{\underline{y}}$	energy release rate density tensor due to debonding and friction
y_{11}, y_{22}, y_{12}	components of the energy release rate density tensor $\underline{\underline{y}}$ in 1-2 frame
Y	cracking energy release rate density
Y_f, Y_{fl}	energy release rate densities associated with fiber-breakage
Y_{f0}, m_f	parameters of the evolution of fiber-breakage damage
Y_i	set of energy release rate densities
Y_m, Y_{my}	energy release rate densities associated with matrix-cracking
:	contraction wrt. two indices

1. Introduction

This study is concerned with the behavior of ceramics reinforced by continuous ceramic fibers. It has been demonstrated by Averston *et al.* (1971) that following matrix-cracking, sliding occurs at the fiber-matrix interface which causes inelastic deformations. The presence of matrix cracks and inelastic deformations may impart to the material the ability to redistribute stresses. In fact the results of experiments on notched panels on SiC/CAS composites (Cady *et al.*, 1995b) suggest the capacity of the material to redistribute stresses is sufficiently high for this material to be notch-insensitive. The ability to redistribute stress is an important property since design studies indicate that working stresses are sufficiently high for matrix-cracking to be unavoidable in regions of stress concentration.

The micromechanics which describes interface debonding and sliding has been established by Hutchinson and Jensen (1990) and Evans *et al.* (1994). In contrast to the early phenomenological studies (Ladevèze, 1983) the intention of the present study is to develop a continuum description of the damage processes which is mechanism-based and which may be used to describe the behavior of Ceramic-Matrix Composites (CMCs) under the conditions of multiaxial stress occurring in practice. Since crack spacing at saturations is small (Beyerley *et al.*, 1992) in most CMCs, Continuum Damage Mechanics is an appropriate means of describing degradation since changes in elastic moduli measured on a macroscopic level provide a simpler and more robust means of measuring damage than does microscopic measurement of crack density, which requires the average of many readings before reliable values are established (Jansson and Leckie, 1993).

By combining Continuum Damage Mechanics (CDM) (Lemaitre, 1992) with the micromechanical studies referred to previously, constitutive equations are developed

which lend themselves to the finite element procedures commonly used in practice (Zienkievicz and Taylor, 1989; Hibbitt *et al.*, 1995). The CDM formulation applied to reinforced composites is written within the framework of the Thermodynamics of Irreversible Processes (Coleman and Gurtin, 1967; Rice, 1971; Germain *et al.*, 1983). The first step in establishing such a model is to identify the internal variables which define the state of the material. The second step is to determine the expression of the state potential in terms of the state variables and the third one to define the evolution laws of the internal variables.

The model is developed along the lines described, for instance, by Ashby (1992). As mentioned earlier, the aim of the model is to be applied to structural applications. The degradation mechanisms are first determined by analyzing unidirectional CMCs in Section 2. The model is then extended to multidirectional systems in Section 3 by modeling the same mechanisms. The procedure described in the previous paragraph constitutes the general framework in which the model is written. In Section 4, the model identification is developed. In particular the number of tests constitutive of the input to the parameter tuning are discussed. The procedure is applied to continuous fiber SiC/SiC composites in a [0/90] lay-up for which suitable experimental data are available (Pluvinage, 1991). Section 5 is concerned with the prediction of a Iosipescu shear experiment. The results are compared with experimental data. This last section constitutes a first validation of the model.

2. The tensile stress-strain relationship for unidirectional CMCs

Post-mortem analyses of broken specimens indicate the presence of arrays of microcracks in the matrix which are accompanied by debonding and friction at the fiber-matrix interface. Hutchinson and Jensen (1990) and Evans *et al.* (1994) have analyzed the behavior of unidirectional CMCs in tension by considering the unit cell shown in Figure 1, when matrix-cracking of spacing $2L$ is accompanied by debonding and sliding at the interface over a friction length $2l_F$. The micromechanics analysis can predict the one-dimensional macroscopic stress-strain response shown in Figure 2. The microcracks are usually aligned with the principal stress or strain directions. By studying a cracked panel with crack of length $2a$ in a cell of area $4LW$ *(Fig. 3)*, the reduction in stiffness may be estimated. If the initial behavior of the elementary cell is isotropic and elastic, and Young's modulus is E, it can be shown that the stiffness loss depends on the crack density defined as $\pi a^2/4LW$. By assuming plane stress conditions, and that the crack interactions can be neglected, a first approximation for the reduced elastic modulus $\widetilde{E}$ can be written as

$$\frac{\widetilde{E}}{E} = \frac{1}{1 + 2\frac{\pi a^2}{4LW}} \tag{1}$$

The relationship can be recast in framework of CDM (Lemaitre and Chaboche, 1978) as

$$\frac{\widetilde{E}}{E} = 1 - D \tag{2}$$

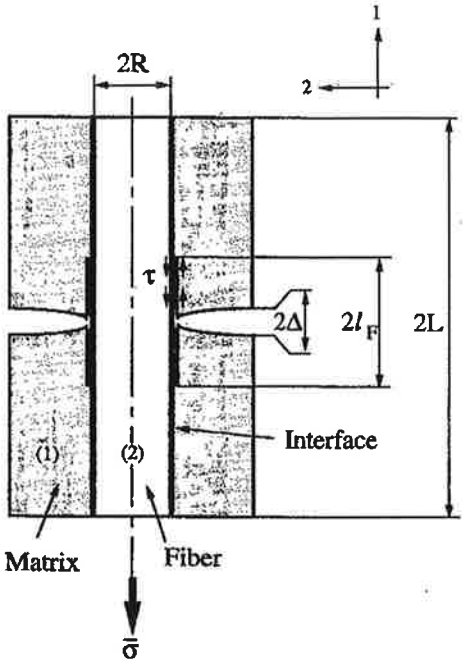

Fig. 1. – Elementary cell containing a crack. A debond zone is characterized by the debond length $2l_F$, and the average crack spacing is $2L$.

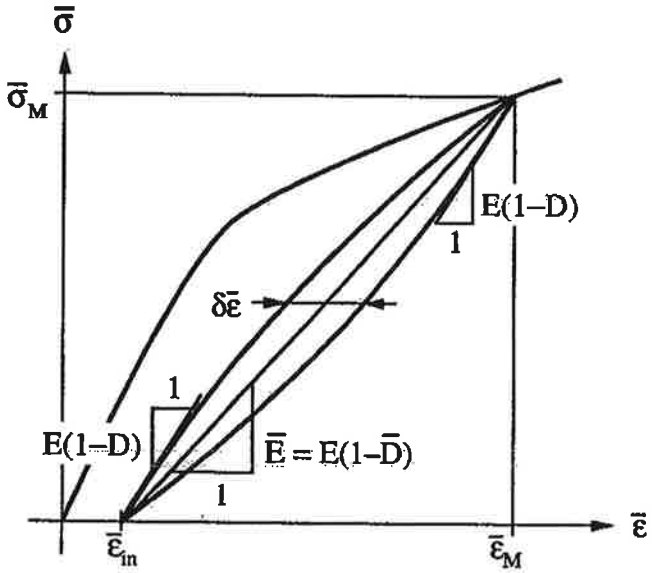

Fig. 2. – Stress, $\bar{\sigma}$, *versus* strain, $\bar{\varepsilon}$, during a loading-unloading-reloading sequence.

where

(3)
$$D = \frac{2\frac{\pi a^2}{4LW}}{1 + 2\frac{\pi a^2}{4LW}}$$

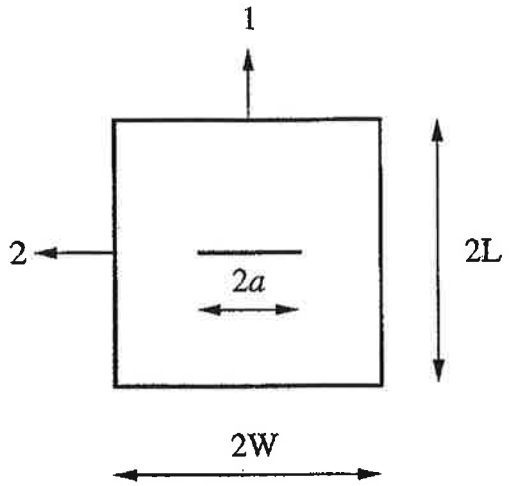

Fig. 3. – Elementary cell of size $2L \times 2W$ containing a crack of size $2a$.

is the damage variable associated with the crack density. When D is small, a first order solution to Eq. (3) is given by

$$D \simeq 2\frac{\pi a^2}{4LW} \tag{4}$$

so that the damage variable is proportional to the crack density. In the case of constituents with different elastic properties, D depends upon the elastic properties of the two constituents, as well as on the geometry (*i.e.*, the ratios a/R and a/L, see *Fig.* 1, where R is the fiber radius). The uniaxial stress-strain relationship becomes

$$\sigma = \frac{\overline{\sigma}}{1-D} = E\,\overline{\varepsilon} \tag{5}$$

The elementary cell illustrated in Figure 1 has been analyzed by various authors (Hutchinson and Jensen, 1990; Evans *et al.*, 1994), but a different analytic approach is now used which follows the thermodynamic developments of Rice (1971) and Germain *et al.* (1983) and which can be formulated conveniently in one and three dimensions alike. This is done by calculating the internal elastic energy density in the unit cell (Hild *et al.*, 1996) caused by matrix-cracking, debonding and sliding at the interface. Two "cut and paste" steps are used to evaluate the elastic energies following approaches introduced by Volterra (1907), and applied to the analysis the elastic behavior of homogeneous and isotropic media by considering the elastic properties of a cut cylinder (Volterra, 1907; Love, 1927), as well as inclusions in an infinite medium (Eshelby, 1957), or to the study creeping materials (Cocks and Leckie, 1987). The first step consists in moving the unbroken part (2) with respect to the broken part (1) with no external load by an amount Δ_s over a length l_F (*Fig.* 4). Because of interfacial sliding, this displacement Δ_s gives rise to a self-balanced linear stress field along a length l_F in parts (1) and (2) when the interfacial behavior is assumed to be characterized by a constant shear strength. By

integration over l_F and then averaging over the total length L, the elastic energy density associated with this process is given by

$$\psi^s = \frac{2}{3}\frac{fE_1(1-f)E_2}{E}\left\{\frac{\Delta_s}{l_F}\right\}^2\frac{l_F}{L} \tag{6}$$

The crack opening displacement Δ_s due to slip induces are irreversible or inelastic strain α expressed as

$$\alpha = \frac{(1-f)E_1}{E}\frac{\Delta_s}{L} \tag{7}$$

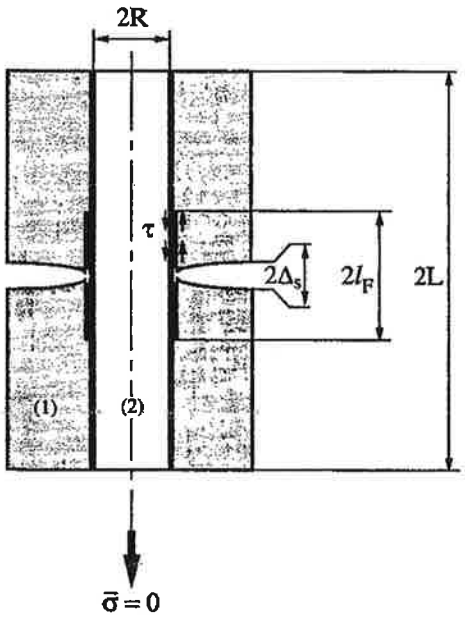

Fig. 4. – Motion of the unbroken part (2) with respect to the broken part (1) with no external load by an amount Δ_s over a length l_F.

The second step consists of an elastic loading of the damaged system so that the elastic energy density is given by

$$\psi^e = \frac{1}{2}E(1-D)(\bar{\varepsilon}-\alpha)^2 \tag{8}$$

The total elastic energy density is the sum of the two elements of the energy densities and that associated with the residual stresses due to processing

$$\psi = \frac{1}{2}E(1-D)(\bar{\varepsilon}-\alpha)^2 + \frac{2}{3}\frac{fE_1(1-f)E_2}{E}\left\{\frac{\Delta_s}{l_F}\right\}^2\frac{l_F}{L} + \rho_1\,\alpha \tag{9}$$

where $-\rho_1 E_1/E$ is the residual stress in the broken layer (1). For convenience the energy density can be expressed in a more compact form by using state variables which

are the total strain $\overline{\varepsilon}$, the damage variable D modeling the loss of stiffness due to the cracking mechanism, the inelastic strain α derived previously (Eq. (7)), and the damage variable $d = 3(1-f)E_1 l_F/4fE_2 L$ which defines the size of the slip zone related to the average crack spacing. The friction length saturates when the cracking process stops ($L = l_F$) along with cracking damage D. Upon loading, all the internal variables vary (since L, l_F and Δ_s evolve), whereas upon unloading, the only variables to vary are the inelastic strain α and d (only Δ changes), D is constant. The elastic energy density in terms of the new internal variables is (Hild *et al.*, 1996)

$$\psi = \frac{1}{2}E(1-D)(\overline{\varepsilon}-\alpha)^2 + \frac{1}{2}E\left(\frac{\alpha^2}{d}\right) + \rho_1\,\alpha. \tag{10}$$

The forces associated with the state variables $(\overline{\varepsilon}, D, d, \alpha)$ are respectively given by

$$\overline{\sigma} = \frac{\partial\psi}{\partial\overline{\varepsilon}} = E(1-D)(\overline{\varepsilon}-\alpha) \tag{11.1}$$

$$Y = -\frac{\partial\psi}{\partial D} = \frac{E}{2}(\overline{\varepsilon}-\alpha)^2 \tag{11.2}$$

$$y = -\frac{\partial\psi}{\partial d} = \frac{E}{2}\left(\frac{\alpha}{d}\right)^2 \tag{11.3}$$

$$X = \frac{\partial\psi}{\partial\alpha} = -\overline{\sigma} + E\frac{\alpha}{d} + \rho_1 \tag{11.4}$$

These associated forces are useful in particular to determine the relevant forces driving each mechanism. Matrix-cracking is assumed to be driven by Y, which plays an identical role as the energy release rate $\mathcal{G}$ in the framework of Linear Elastic Fracture Mechanics. From a micromechanical analysis (Hild *et al.*, 1996), it can be shown that the back-stress is dependent on the applied stress $\overline{\sigma}$, therefore the driving force of the inelastic strains can be taken as the stresses acting in the same direction. The same assumption can be made when the evolution of the damage variable d related to sliding is analyzed, *i.e.* the driving force of d can be chosen to be its associated force y, or the applied stress $\overline{\sigma}$.

In the present approach the growth laws of the internal variables (D, d, α) are established from macroscopic quantities measured in the course of unloading and reloading sequences. To this end use is made of the solution of the response of the unit cell (*Fig.* 1) when subjected to an unloading/reloading sequence during which the magnitude of the shear stress remains constant.

The expressions obtained from the analysis for the residual stress ρ_1 and the internal variables D, d, α in terms of the macroscopic quantities shown in Figure 2 are given respectively by (Hild *et al.*, 1996).

$$\frac{-\rho_1}{E} = \left(\sqrt{\frac{\overline{\varepsilon}_{\text{in}} + 2\delta\overline{\varepsilon}}{4\delta\overline{\varepsilon}}} - 1\right)(\overline{\varepsilon}_M - \overline{\varepsilon}_{\text{in}} - 2\delta\overline{\varepsilon}) \tag{12.1}$$

$$D = \frac{\overline{\varepsilon}_M\overline{D} - \overline{\varepsilon}_{\text{in}}\overline{D} - 2\delta\overline{\varepsilon}}{\overline{\varepsilon}_M - \overline{\varepsilon}_{\text{in}} - 2\delta\overline{\varepsilon}} \tag{12.2}$$

(12.3) $$\frac{d}{4} = \frac{\sqrt{(\bar{\varepsilon}_{\text{in}} + 2\delta\bar{\varepsilon})\delta\bar{\varepsilon}}}{\bar{\varepsilon}_M - \bar{\varepsilon}_{\text{in}} - 2\delta\bar{\varepsilon}}$$

(12.4) $$\alpha = \frac{d}{2}\frac{\bar{\sigma}_M - \rho_1(1-D)}{E(1-D)}$$

Equations (12) are only valid when a constant shear strength characterizes the interfacial behavior, and lastly Eqs. (12.3) and (12.4) are only valid for monotonic loading conditions.

By performing a series of unloading/reloading sequences the internal variables can be determined from experiment using Eqs. (12). The residual stress ρ_1 is calculated from Eq. (12.1) and it is a test of the effectiveness of the model that the same value of the residual stress is obtained for each loading sequence. The values of D and d are given by applying Eqs. (12.2) and (12.3) respectively. The information is now available to complete the calculation for Eq. (12.4). The corresponding associated forces are obtained by the expressions givens in Eqs. (11). The relationship between the internal variables and the associated forces can then be investigated by knowing the driving forces of each state variable. This method is proposed to model the behavior of CMC laminates.

3. CMCs with multidirectional fiber systems

The one-dimensional investigation is now extended to a [0/90] laminate composite and to a [0/90] woven composite subjected to multiaxial plane stress states. In this paper, only monotonic loading conditions are analyzed, even though the present framework can be easily extended to cyclic loading conditions and to non-proportional loading conditions. Following established procedures, the properties of each layer are first determined and those of the composite are then calculated by ensuring compatibility conditions.

The components of each layer consist of the matrix, the fiber and the interface, with f being the fiber volume fraction. The fiber direction defines the 1-2 axes. The axes x-y correspond to the principal axes of the strains in the ceramic matrix. The definition of the axes used at the constituent, layer and composite levels are shown in Figure 5. Following Section 2, the loss of stiffness due to matrix-cracking and fiber-breakage is first established and this is followed by the influence of the slip at the interfaces.

3.1. Elastic energies of the composite associated with matrix-cracking and fiber-breakage

3.1.1. *Constituent level: matrix and fiber*

The initial behavior of the matrix is assumed to be isotropic. The presence of cracks leads the behavior to become anisotropic. The assumption is made that cracking occurs normal to the y-direction (e.g. maximum principal strain direction) in the matrix. Under the hypothesis of monotonic loading condition, only one damage variable is needed to

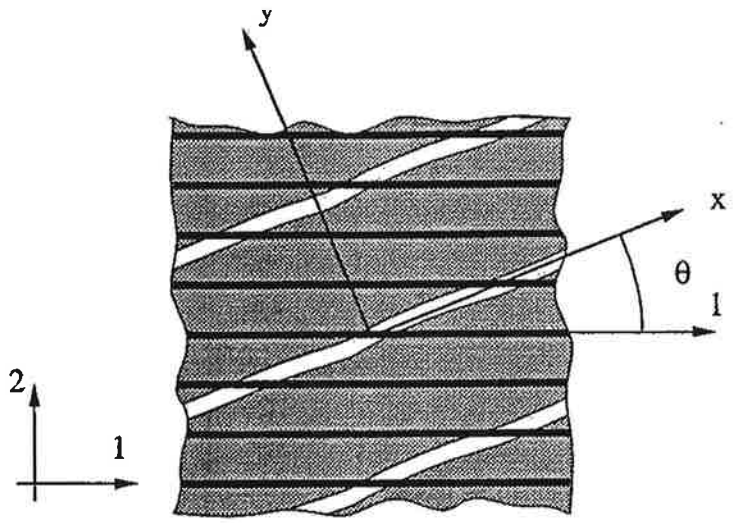

Fig. 5. – The initial principal directions of orthotropy, or material directions, 1 and 2 often do not coincide with the loading directions x and y. The angle θ measures their respective orientation.

model matrix-cracking, and is denoted by D_{my}. The study of a cracked system normal to one direction shows that the Young's modulus along that direction as well as the shear modulus are altered (Budiansky and O'Connell, 1976; Chaboche, 1982) and that the expression of the elastic energy density of the matrix is

$$\psi_m = \frac{1}{2}\frac{E_m(\varepsilon_{mxx}^2 + 2\nu_m(1-D_{my})\varepsilon_{mxx}\varepsilon_{myy} + (1-D_{my})\varepsilon_{myy}^2)}{1-\nu_m^2(1-D_{my})} + 2\tilde{G}_m(D_{my})\varepsilon_{mxy}^2 \tag{13.1}$$

and

$$\tilde{G}_m(D_{my}) = \frac{G_m}{1+\left(\frac{D_{my}}{1-D_{my}}\right)\frac{1}{2(1+\nu_m)}}$$

It is assumed that the fibers are aligned along the 1-direction and that fiber-breakage is perpendicular to the fiber direction. Therefore the elastic energy density is given by

$$\psi_f = \frac{1}{2}(E_f(1-D_{f1})\varepsilon_{f11}^2 + E_f\varepsilon_{f22}^2) + 2\tilde{G}_f(D_{f1})\varepsilon_{f12}^2 \tag{13.2}$$

The expression of the stresses in the matrix $\underline{\underline{\sigma}}_m$ and in the fibers $\underline{\underline{\sigma}}_f$ are obtained by partial differentiation of the elastic energy density with respect to the strain tensors $\underline{\underline{\varepsilon}}_m$ and $\underline{\underline{\varepsilon}}_f$ respectively

$$\underline{\underline{\sigma}}_m = \frac{\partial \psi_m}{\partial \underline{\underline{\varepsilon}}_m} \tag{14.1}$$

$$\underline{\underline{\sigma}}_f = \frac{\partial \psi_f}{\partial \underline{\underline{\varepsilon}}_f} \tag{14.2}$$

and the associated forces to the damage variables are defined as

$$Y_{my} = -\frac{\partial \psi_m}{\partial D_{my}} \tag{14.3}$$

$$Y_{f1} = -\frac{\partial \psi_f}{D_{f1}} \tag{14.4}$$

These generalized forces are the energy release rate densities associated with matrix-cracking and fiber-breakage, respectively. They play similar roles as the force Y introduced in Section 2, and therefore are assumed to be the driving forces of the damage variables.

3.1.2. *Layered composite*

When the composite consists of layers of unidirectional fibers with different orientations, the laminate properties are determined by applying laminate theory to the properties of individual layers.

3.1.2.1. Layer level

A layer consists of fibers aligned along one orientation (the 1-direction) embedded in a matrix. To determine the behavior of this layer, micro-interface compatibility conditions are written in terms of the strains $\underline{\underline{\varepsilon}}^L$ and stresses $\underline{\underline{\sigma}}^L$ on the layer level. These conditions are the compatibility and the equilibrium between a fiber (tensors $\underline{\underline{\varepsilon}}_f$ and $\underline{\underline{\sigma}}_f$) and the surrounding matrix (tensors $\underline{\underline{\varepsilon}}_m$ and $\underline{\underline{\sigma}}_m$), which takes place in that system. Therefore, it is more convenient to write the conditions in the 1-2 material frame as follows,

$$\varepsilon_{m11} = \varepsilon_{f11} = \varepsilon^L_{11} \tag{15.1}$$

$$f_m \sigma_{m11} + f_f \sigma_{f11} = \sigma^L_{11} \tag{15.2}$$

$$f_m \varepsilon_{m22} + f_f \varepsilon_{f22} = \varepsilon^L_{22} \tag{15.3}$$

$$\sigma_{m22} = \sigma_{f22} = \sigma^L_{22} \tag{15.4}$$

$$f_m \varepsilon_{m12} + f_f \varepsilon_{f12} = \varepsilon^L_{12} \tag{15.5}$$

$$\sigma_{m12} = \sigma_{f12} = \sigma^L_{12} \tag{15.6}$$

When the principal strain directions do not coincide with the material frame, Eqs. (14.1-14.2) have to be rewritten in the 1-2 frame. The application of Eqs. (15) then defines

the elastic properties of the layer

$$\underline{\underline{\sigma}}^{L} = \underline{\underline{\underline{\underline{E}}}}^{L}\left(D_{my}, D_{f1}\right) : \underline{\underline{\varepsilon}}^{L} \tag{16.1}$$

From Eq. (16.1), the elastic energy density ψ^L associated with matrix-cracking and fiber-breakage on the layer level can be written as

$$\psi^{L} = \frac{1}{2}\,\underline{\underline{\varepsilon}}^{L} : \underline{\underline{\underline{\underline{E}}}}^{L}\left(D_{my}, D_{f1}\right) : \underline{\underline{\varepsilon}}^{L} \tag{16.2}$$

Matrix-cracking and fiber-breakage are dissipative mechanisms which do not store energy. Therefore they influence only the reversible (*i.e.*, elastic) part of the free energy density.

3.1.3. *Composite level*

For simplicity, the case of two layers at 0 and 90 degrees are considered. The micromechanical quantities associated with the 0 degree layer are superscripted by ^{00}, and those at 90 degrees by ^{90}. The elastic behavior of the composite system is determined by applying classical laminate theory. The compatibility condition and global equilibrium allow to get the overall stresses $\underline{\underline{\sigma}}$ and strains $\underline{\underline{\varepsilon}}$

$$\underline{\underline{\varepsilon}} = \underline{\underline{\varepsilon}}^{00} = \underline{\underline{\varepsilon}}^{90} \tag{17.1}$$

$$\underline{\underline{\sigma}} = f^{00}\underline{\underline{\sigma}}^{00} + f^{90}\underline{\underline{\sigma}}^{90} \tag{17.2}$$

By solving Eqs. (17) and using Eq. (16.1), the overall behavior of the composite is defined as

$$\underline{\underline{\sigma}} = \underline{\underline{\underline{\underline{E}}}}\left(D_{my}^{00}, D_{my}^{90}, D_{f1}^{00}, D_{f1}^{90}\right) : \underline{\underline{\varepsilon}} \tag{18.1}$$

with

$$\underline{\underline{\underline{\underline{E}}}}\left(D_{my}^{00}, D_{my}^{90}, D_{f1}^{00}, D_{f1}^{90}\right) = f^{00}\underline{\underline{\underline{\underline{E}}}}\left(D_{my}^{00}, D_{f1}^{00}\right) + f^{90}\underline{\underline{\underline{\underline{E}}}}\left(D_{my}^{90}, D_{f1}^{90}\right)$$

From Eq. (18.1), the elastic energy density ψ^D associated with matrix-cracking and fiber-breakage on the composite level can be written as

$$\psi^{D} = f^{00}\psi^{00} + f^{90}\psi^{90} \tag{18.2}$$

with

$$\psi^{00} = \frac{1}{2}\underline{\underline{\varepsilon}} : \underline{\underline{\underline{\underline{E}}}}^{00}\left(D_{my}^{00}, D_{f1}^{00}\right) : \underline{\underline{\varepsilon}} \tag{18.3}$$

$$\psi^{90} = \frac{1}{2}\underline{\underline{\varepsilon}} : \underline{\underline{\underline{\underline{E}}}}^{90}\left(D_{my}^{90}, D_{f1}^{90}\right) : \underline{\underline{\varepsilon}} \tag{18.4}$$

3.1.2. *Woven composite*

Woven composites are another architecture commonly used. Equations (16) can be used also for woven architectures. This approximation is relevant when two different damage mechanisms can be exhibited in the tows at 0 and 90 degrees. Also, the effects due to fiber cross-over are neglected. Therefore the results developed so far can be extended to woven architectures.

However, there may be some situations in which the distinction between the matrix of the tows at 0 and 90 degrees is more difficult to make because there is only one matrix-cracking mechanism. In place of Eq. (16) for the single layer, the equilibrium and compatibility conditions are given by the following equations written in the 1-2 frame

$$\varepsilon_{m11} = \varepsilon_{f11}^{1} = \varepsilon_{11} \tag{19.1}$$

$$\sigma_{m11} = \sigma_{f11}^{2} \tag{19.2}$$

$$(1 + f_m)\sigma_{m11} + f_f\sigma_{f11}^{1} = 2\sigma_{11} \tag{19.3}$$

$$\varepsilon_{m22} = \varepsilon_{f22}^{2} = \varepsilon_{22} \tag{19.4}$$

$$\sigma_{m22} = \sigma_{f22}^{1} \tag{19.5}$$

$$(1 + f_m)\sigma_{m22} + f_f\sigma_{f22}^{2} = 2\sigma_{22} \tag{19.6}$$

$$f_m\varepsilon_{m12} + f_f\varepsilon_{f12}^{1} = \varepsilon_{12} \tag{19.7}$$

$$\sigma_{m12} = \sigma_{f12}^{1} = \sigma_{f12}^{2} = \sigma_{12} \tag{19.8}$$

By solving Eqs. (19) and noting that there exists only one degradation mechanism taking place in the matrix characterized by one damage variable D_{my} and two

degradation mechanisms associated with fiber-breakage in the 0 and 90 degrees directions $\left(D_{f1}^{00}, D_{f1}^{90}\right)$, the overall behavior of the composite is defined as

$$\underline{\underline{\sigma}} = \underline{\underline{\underline{\underline{E}}}}\left(D_{my}, D_{f1}^{00}, D_{f1}^{90}\right) : \underline{\underline{\varepsilon}} \tag{20.1}$$

The elastic energy density ψ^D associated with matrix-cracking and fiber-breakage on the composite level can be written as

$$\psi^D = \frac{1}{2}\,\underline{\underline{\varepsilon}} : \underline{\underline{\underline{\underline{E}}}}\left(D_{my}, D_{f1}^{00}, D_{f1}^{90}\right) : \underline{\underline{\varepsilon}} \tag{20.2}$$

3.2. State potential associated with debonding and fiber pull-out

Inelasticity is essentially due to sliding at the interface between the fiber and the matrix. Sliding is involved in debonding as well as fiber pull-out. From a micromechanical point of view, this sliding can take place as soon as a crack is bridged by fibers. In a CDM formulation, only the equivalent homogenous sliding and the associated forces are considered. By considering equivalent homogeneous sliding on the composite level, there is no way to distinguish the contributions due to fiber/matrix debonding and sliding, and inter-layer delamination. However, in most CMCs delamination is not as critical as in polymeric matrix composites for which the Young's moduli differences are far more important. Therefore, the cell model used to describe cracking and sliding is that shown in Figure 1. The analysis that has been done on a 1-D model (given in Section 2) can be formally extended to give the expression of the elastic energy density due to sliding of a layered composite along the 1-2 directions (Burr *et al.*, 1995)

$$\psi^S\left(\underline{\underline{\alpha}}, \underline{\underline{d}}\right) = \frac{1}{2}\,\overline{E}\left(\frac{\alpha_{11}^2}{d_{11}} + \frac{\alpha_{22}^2}{d_{22}}\right) + \frac{1}{2}\,\overline{G}\left(\frac{\alpha_{12}^2}{d_{12}}\right) \tag{21}$$

with

$$\overline{E} = \frac{f^{00}E^{00}f^{90}E^{90}}{f^{00}E^{00} + f^{90}E^{90}}$$
$$\overline{G} = \frac{f^{00}G^{00}f^{90}G^{90}}{f^{00}G^{00} + f^{90}G^{90}}$$

3.2.1. *State laws*

The following development deals with layered CMCs. By using the results of Section 2, the total elastic energy density of the composite is the sum of the elastic energy density of the damaged composite ψ^D and the elastic energy density due to debonding and sliding ψ^S

$$\psi = \frac{1}{2}\left(\underline{\underline{\varepsilon}} - \underline{\underline{\alpha}}\right) : \underline{\underline{\underline{\underline{E}}}}\left(D_{my}^{00}, D_{my}^{90}, D_{f1}^{00}, D_{f1}^{90}\right) : \left(\underline{\underline{\varepsilon}} - \underline{\underline{\alpha}}\right) + \psi^S\left(\underline{\underline{\alpha}}, \underline{\underline{d}}\right) \tag{22}$$

The force associated with total strain is

$$\underline{\underline{\sigma}} = \frac{\partial \psi}{\partial \underline{\underline{\varepsilon}}} = \underline{\underline{\underline{\underline{E}}}}\left(D_{my}^{00}, D_{my}^{90}, D_{f1}^{00}, D_{f1}^{90}\right) : \left(\underline{\underline{\varepsilon}} - \underline{\underline{\alpha}}\right) \tag{23.1}$$

and corresponds to the macrocsopic stress. The associated force to the damage variables modeling matrix-cracking and fiber-breakage are

$$Y_i = -\frac{\partial \psi}{\partial D_i} \tag{23.2}$$

where $D_{i=1;4} = \left\{D_{my}^{00}; D_{my}^{90}; D_{f1}^{00}; D_{f1}^{90}\right\}$, and $Y_{i=1;4} = \left\{Y_{my}^{00}; Y_{my}^{90}; Y_{f1}^{00}; Y_{f1}^{90}\right\}$ represent the corresponding energy release rate densities due to matrix-cracking and fiber-breakage. The associated force to the damage variables modeling sliding are

$$\underline{\underline{y}} = -\frac{\partial \psi}{\partial \underline{\underline{d}}} = -\frac{\partial \psi^S}{\partial \underline{\underline{d}}} \tag{23.3}$$

where $\underline{\underline{d}} = \{d_{11}; d_{22}; d_{12}\}$, and $\underline{\underline{y}}$ correspond to the energy release rate densities due to debonding and sliding. The associated forces to the inelastic strains $\underline{\underline{\alpha}}$ are

$$\underline{\underline{X}} = \frac{\partial \psi}{\partial \underline{\underline{\alpha}}} = -\underline{\underline{\sigma}} + \frac{\partial \psi^S}{\partial \underline{\underline{\alpha}}} \tag{23.4}$$

and represent the back-stresses in the sliding zone. It is worth noting that in this section the residual stresses are not accounted for. Otherwise there would have been an additional term in Eqs. (23.4) and (22).

3.2.2. *Evolution laws*

The identification procedure is performed on a $[0/90]_s$ laminate architecture of CMCs. The first step is to define all the internal state variables needed to model the material behavior. The three total strain variables, (e.g., $\varepsilon_{11}, \varepsilon_{22}, \varepsilon_{12}$), are given either from experiment or as input from a F.E. calculation. The four damage variables $D_{i=1;4} = \left\{D_{my}^{00}; D_{my}^{90}; D_{f1}^{00}; D_{f1}^{90}\right\}$ are used to define the change in the elastic properties, with $D_m = \left\{D_{my}^{00}; D_{my}^{90}\right\}$ is the set of damage variables modeling matrix-cracking, and $D_f = \left\{D_{f1}^{00}; D_{f1}^{90}\right\}$ is the set of damage variables modeling fiber-breakage. Assuming the damage evolution laws, $D_m(Y_m)$ and $D_f(Y_f)$ are functions of the associated forces $Y_m = \left\{Y_{my}^{00}; Y_{my}^{90}\right\}$, and $Y_f = \left\{Y_{f1}^{00}; Y_{f1}^{90}\right\}$ respectively, then only two evolution laws, one for each mechanism, are sufficient to compute the four components or damage. The three damage variables, $\{d_{11}; d_{22}; d_{12}\}$, define the sliding distances, with d_{11} or d_{22} being associated with sliding in the fiber directions and d_{12} associated with shear sliding. Consequently only two evolution laws are needed, $d_{11}(y_{11})$ or $d_{22}(y_{22})$, and $d_{12}(y_{12})$.

For the same reasons, two evolution laws for the inelastic strains, $\alpha_{11}(X_{11})$ or $\alpha_{22}(X_{22})$, and $\alpha_{12}(X_{12})$ define the evolution of the three inelastic strains, $\{\alpha_{11}; \alpha_{22}; \alpha_{12}\}$. In conclusion, the model has 13 state variables, three of which are

TABLE I. – Thermodynamic variables modeling elasticity, matrix cracking, debonding and sliding, fiber breakage and pull-out.

Mechanism	State variables			Associated forces	
		Observable	Internal		
Elasticity	Total strain	$\underline{\underline{\varepsilon}}$		$\underline{\underline{\sigma}}$	Stress
Matrix-cracking	Damage variables		D_m^{00} D_m^{90}	Y_m^{00} Y_m^{90}	Energy release rate densities
Fiber-breakage	Damage variables		D_f^{00} D_f^{90}	Y_f^{00} Y_f^{90}	Energy release rate densities
Debonding and sliding	Inelastic strain		$\underline{\underline{\alpha}}$	$\underline{\underline{X}}$	Back-stress
	Damage variables		d_{11} d_{22} d_{12}	y_{11} y_{22} y_{12}	Energy release rate densities

strain inputs and the remaining 10 micromechanical internal variables are derived from 6 evolution laws. Therefore, the set S of state variables is (*Table* 1)

$$S = \left\{\underline{\underline{\varepsilon}}; \underline{\underline{\alpha}}; D_{i=1;4}; \underline{d}\right\} \tag{24.1}$$

and the associated forces F are (*Table* 1)

$$F = \left\{\underline{\underline{\sigma}}; \underline{\underline{X}}; Y_{i=1;4}; \underline{y}\right\} \tag{24.2}$$

The second step is to define the relevant tests required to identify the growth of the six internal variables. This is achieved from unloading/reloading tests performed at regular intervals and measuring the macroscopic inelastic strain upon complete unloading, $\overline{\varepsilon}_{\text{in}}$, the macroscopic damage of the composite, $\overline{D}$, and the maximum hysterisis loop width, $\delta\overline{\varepsilon}$ (*Fig.* 2). Using Eqs. (12), the internal variables can be calculated.

When tension is applied at 45 degrees on a $[0/90]_s$ layered composite, the macroscopic damage variable, $\overline{D}^{45}$, is related to the microscopic damage variables taking place in the matrix alone, $\left\{D_{my}^{00}, D_{my}^{90}\right\}$, by using the transformation rules given in the Appendix. Moreover, in this particular case, the two damage variables D_{my}^{00} and D_{my}^{90} have the same value. Therefore, the evolution law, $D_m(Y_m)$, is directly given by the evolution of the macroscopic damage of the composite $\overline{D}^{45}$ (*Fig.* 6).

The evolution law of the damage variable associated with fiber-breakage, $D_f\left(Y_f\right)$, is found from measurement of the macroscopic damage $\overline{D}^{00}$ (*Fig.* 6) in a tension test at 0 degree on the [0/90] which has been compensated by the contribution matrix-cracking which is calculated from the results of the first test.

Similarly, the evolution laws of the state variables related to sliding, $\alpha_{11}(X_{11})$ or $\alpha_{22}(X_{22})$, and $d_{11}(y_{11})$ or $d_{22}(y_{22})$ are known from the evolution of the macroscopic

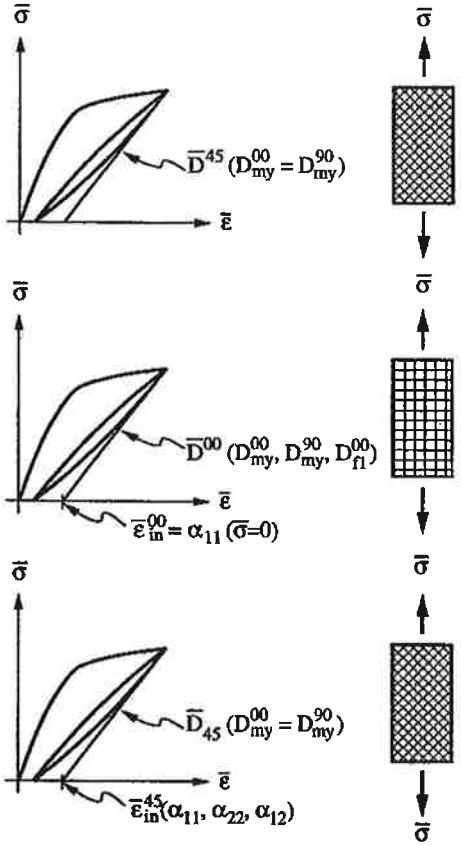

Fig. 6. – Flow chart of the identification procedure.

inelastic strain upon complete unloading $\bar{\varepsilon}_{\text{in}}^{00} = \alpha_{11}(\bar{\sigma}_{11} = 0)$, the macroscopic damage of the composite, $\overline{D}^{00}$, and the maximum hysteresis loop width, $\delta\bar{\varepsilon}^{00}$, using generalized micromechanics relations (Eqs. 12)

$$\frac{-\rho_1^{00}}{E^{00}} = \left(\sqrt{\frac{\bar{\varepsilon}_{\text{in}}^{00} + 2\delta\bar{\varepsilon}^{00}}{4\delta\bar{\varepsilon}^{00}}} - 1\right)(\bar{\varepsilon}_m^{00} - \bar{\varepsilon}_{\text{in}}^{00} - 2\delta\bar{\varepsilon}^{00}) \tag{25.1}$$

$$D^{00} = \frac{\bar{\varepsilon}_M^{00}\overline{D}^{00} - \bar{\varepsilon}_{\text{in}}^{00}\overline{D}^{00} - 2\delta\bar{\varepsilon}^{00}}{\bar{\varepsilon}_M^{00} - \bar{\varepsilon}_{\text{in}}^{00} - 2\delta\bar{\varepsilon}^{00}} \tag{25.2}$$

$$\frac{d_{11}}{4} = \frac{\sqrt{(\bar{\varepsilon}_{\text{in}}^{00} + 2\delta\bar{\varepsilon}^{00})\delta\bar{\varepsilon}^{00}}}{\bar{\varepsilon}_M^{00} - \bar{\varepsilon}_{\text{in}}^{00} - 2\delta\bar{\varepsilon}^{00}} \tag{25.3}$$

$$\alpha_{11} = \frac{d_{11}}{2}\,\frac{\bar{\sigma}_M^{00} - \rho_1^{00}(1 - D^{00})}{E^{00}(1 - D^{00})} \tag{25.4}$$

Finally, returning to the results of the tension test at 45 degrees on a $[0/90]_s$ layered composite (*Fig.* 6), the evolution laws of the state variables related to sliding, $\alpha_{12}(X_{12})$

and $d_{12}(y_{12})$ are given by the following relationships similar to those calculated by the micromechanical analysis

$$\frac{d_{12}}{4} = \frac{\overline{\varepsilon}_{\text{in}}^{45}}{\overline{\varepsilon}_{M}^{45} - 2\overline{\varepsilon}_{\text{in}}^{45}} \tag{26.1}$$

$$\alpha_{12} = \frac{d_{12}}{2} \frac{\overline{\varepsilon}_{M}^{45}}{1 + \frac{d_{12}}{2}} \tag{26.2}$$

In this analysis, it can be noticed that the residual stress $-\rho_1^{45}$ in the tension direction is equal to zero, and therefore $\overline{\varepsilon}_{\text{in}}^{45} = 2\delta\overline{\varepsilon}^{45}$, which leads to the above results. Equations (25) and (26) can be used to predict the overall behavior of the analyzed CMC. However, they are valid provided the interfacial behavior can solely be modeled by a constant interfacial shear strength. This is not the only model available to study CMCs. Therefore the evolution laws of the damage variables as well as the inelastic strains are determined by direct measurement of their values at different stress levels. The drawback of this approach is that the model is not completely identified since the damage variables related to debonding and sliding are not identified. Therefore the part of the free energy that is stored is not fully determined since it depends upon the details of the interfacial behavior. The stress/strain relationship however is known and thus a structural analysis can be performed.

In summary, only two tests, on the same architecture, enable us to extract all six evolution laws that define the behavior of the material (see *Fig.* 6). Two tensile tests are sufficient when the back-stresses are computed (therefore the damage variables related to debonding and sliding). In the following it will be shown that two tests are still sufficient as long as the evolution of the inelastic strain α_{12} can be obtained by the analysis of one of the tensile tests.

4. Model identification

The identification is performed on a $[0/90]_s$ laminate architecture of a SiC/SiC composite using the experimental results of Pluvinage (1991). Only two tension tests are used to establish the evolution laws of the damage quantities and the inelastic strains. The first step is to consider the elastic properties. Inspection of the composite (Pluvinage, 1991) indicates the presence of porosity in the matrix. Because the model is mechanism-based, the only means of accounting for this porosity is by an initial non-zero matrix damage quantity, D_{m0}. The measurement of Young's Moduli E^{00} and E^{45} respectively for a 0 degree and $\pm$ 45 degree tension tests combined with their analytic expressions gives the value of the initial non-zero isotropic damage quantity, $D_{m0} = 0.7$, which affects *only the initial elastic properties*. This damage value is consistent with experimental observations of initial porosities due to the Chemical Vapor Infiltration technique used to process these materials (Pluvinage, 1991).

The evolution laws of the state variables are written in terms of the associated forces. Therefore, the evolution of the damage variables is written as a function of the strain energy release rate densities. The evolution of the inelastic strains is written in terms of the corresponding back-stresses. It can be shown that the back-stresses are linearly proportional to the macroscopic stresses as shown in Eqs. (23.4) and (25.4). For the sake of simplicity, the evolution of the inelastic strains is thus written in terms of the macroscopic stresses. Lastly, the evolution of the damage variable $\underline{\underline{d}}$ is not explicitly needed in the present approach since only monotonic loading conditions are considered (*see* Section 2) and no particular statement is made concerning the interfacial behavior (*see* Section 3).

From the analysis of a tension test at 0 degree, the maximum hysteresis loop width is close to half of the corresponding inelastic strain upon complete unloading. It is concluded from Eq. (25.1) that the macroscopic residual stresses are very small and will therefore be neglected.

The variation of D_m with Y_m obtained from the experimental data is shown in Figure 7 a. Since matrix cracking is related to the presence of randomly distributed flaws, an appropriate form of evolution law which can fit the data shown in Figure 7 a is given by a Weibull law (1939; 1951)

$$D_m = D_{sat}\left(1 - \exp\left[-\left(\frac{Y_m - Y_{mth}}{Y_{m0}}\right)^{m_m}\right]\right) \tag{27}$$

The values that fit the data of Figure 7 a are

$$D_{sat} = 1.0 \quad Y_{mth} = 0\,\mathrm{Jm}^{-3} \quad Y_{m0} = 0.6\,\mathrm{Jm}^{-3} \quad m_m = 1.2 \tag{28}$$

The threshold energy release rate density Y_{mth} has a zero value in accordance with the hypothesis of no macroscopic residual stresses. The parameters Y_{m0} and m_m are directly related to the evolution of cracking density as a function of applied stress. The damage parameter at saturation has a very high value in agreement with the fact that average crack spacing is very small for these composites (Pluvinage, 1991). The evolution laws for matrix damage having been determined, the fiber-breakage damage D_f can be plotted, as a function of Y_f. Using Curtin's relationship (1991) for fiber damage, the evolution law is given by

$$D_f = 1 - \exp\left[-\left(\frac{Y_f}{Y_{f0}}\right)^{(m_f+1)/2}\right] \tag{29}$$

In the following computations, it was assumed that during the matrix-cracking process, only few fibers break. Therefore, no attempt was made to identify the previous parameters.

Lastly, the expression used to fit the evolution laws for the inelastic strains shown in Figures 7 b and 7 c are

$$\alpha_i = \frac{\langle \sigma_i - \sigma_{th} \rangle}{\sigma_0} \tag{30}$$

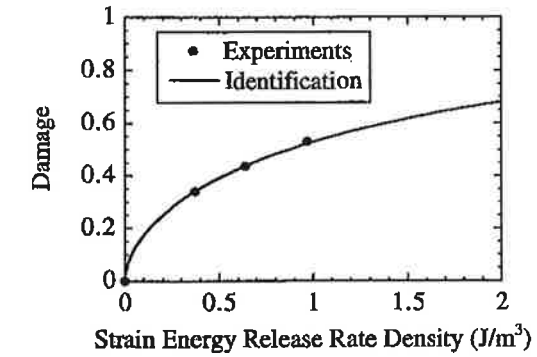

(a)

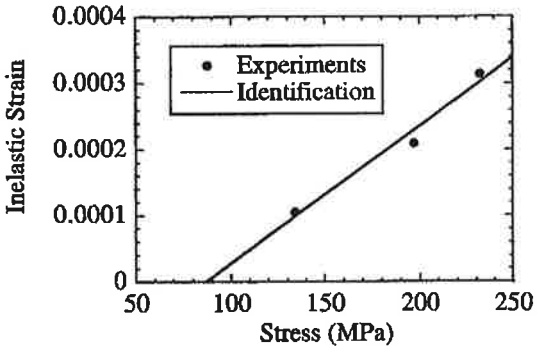

(b)

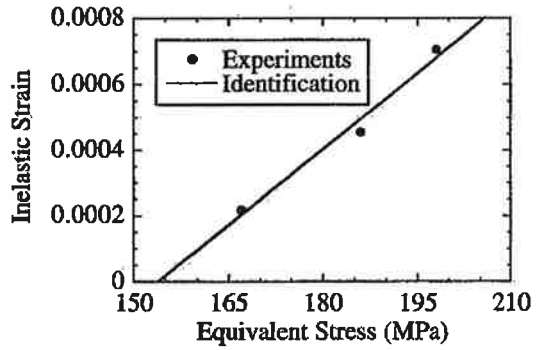

(c)

Fig. 7. – Experimental and identified evolution of:
(a) the matrix-cracking damage variable D_m as a function of the strain energy release rate density associated with matrix-cracking Y_m;
(b) the inelastic strains α_{11} (or α_{22}) as a function of the stress σ_{11} (or σ_{22});
(c) the inelastic strains α_{12} as a function of the equivalent stress τ_{eq}.

$$\alpha_{12} = \frac{\langle \tau_{eq} - \tau_{th} \rangle}{\tau_0} \mathrm{Sign}(\sigma_{12}) \tag{31}$$

The material parameters of Eqs. (30) and (31) are related to the interfacial behavior.

The introduction of the expression for τ_{eq} comes from the observation that the stress/strain curves obtained for tensile tests at ± 45 degrees and shear tests at 0 degree almost coincide for CMC systems. This observation appears to apply for a whole class of materials: SiC/SiC, SiC/CAS, SiC/C, C/C composites (Cady *et al.*, 1995*a*), and

presumably SiC/Al_2O_3 composites (Heredia *et al.*, 1995). One choice for τ_{eq} which satisfies this requirement is given by

$$\tau_{eq} = \sqrt{\left| \sigma_{12}\left[\sigma_{12} + \frac{3}{2}(\sigma_{11} + \sigma_{22})\right] \right|} \tag{32}$$

Similar behavior is observed in concrete for which both the hydrostatic and shear stress states influence the inelastic deformations (Drucker and Prager, 1956). The definition of the equivalent shear stress given in Eq. (32) enables us to identify all the evolution laws by analyzing two tensile tests. This hypothesis is crucial and will be checked in Section 5. The constants in Eqs. (30) and (31) which define the inelastic strains are given by (see *Fig.* 7 b and 7 c).

$$\begin{aligned} \sigma_{th} &= 88\,\text{MPa} \quad \sigma_0 = 480\,\text{GPa} \\ \tau_{th} &= 154\,\text{MPa} \quad \tau_0 = 64.8\,\text{GPa} \end{aligned} \tag{33}$$

This model is implemented in the industrial Finite Element code ABAQUS (Hibbit *et al.*, 1995) via a user material (UMAT) routine. This allows to investigate more complex loading conditions on a structural level. The Finite Element procedure was checked by analyzing pure tension tests at 0 and $\pm$ 45 degrees. The comparisons in terms of stress-strain between the experiments and the computations are shown in Figure 8. There is a good agreement between the model and the experiments used to identify the model.

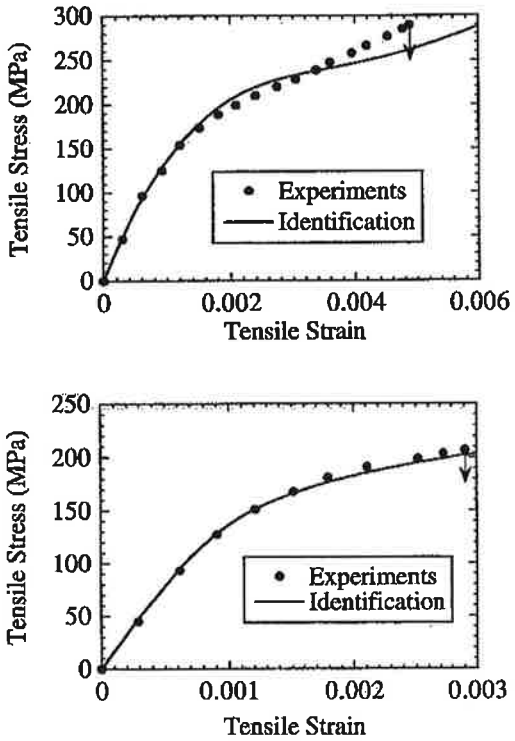

Fig. 8. – Experimental and identified evolution of the tensile stresses σ_{yy} as a function of the tensile strains ϵ_{yy} in
(a) a tension test on a [0/90] SiC/SiC lay-up at 0 degree,
(b) a tension test on a [0/90] SiC/SiC lay-up at $\pm$ 45 degrees.

5. Analysis of experiments on SiC/SiC composites

When the availability of materials is restricted to planar form, the most usual means of obtaining shear data is to subject the Iosipescu specimen (Iosipescu, 1967) to shear force (Pluvinage, 1991). In order to investigate the suitability of the Iosipescu test as a means of obtaining shear data, a Finite Element analysis has been performed using the constitutive equations described and identified previously. The Iosipescu specimen shown in Figure 9 is subjected to shear loading and measurement of the shear properties of the material are obtained by plotting the average stress at the minimum section against the shear strain measured by strain gauges placed at the center of the specimen. It is known that the shear stress at the minimum section of this specimen is sensibly constant when the material is elastic and isotropic, but is is not known if the constant shear stress assumption is valid when cracking occurs. In addition to verifying the suitability of the Iosipescu specimen, the tests provide an opportunity to measure the ability of the constitutive equations to predict the behavior of a component in which the stress state is different from those used in the identification procedure.

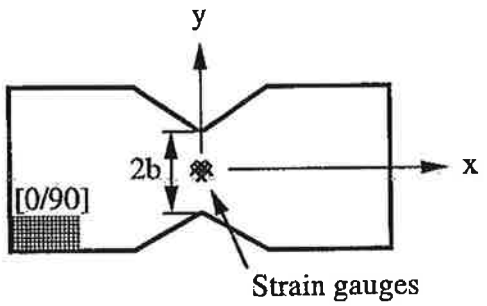

Fig. 9. – Iosipescu specimen configuration.

The plot of the average stress against the strain at the center of the specimen is shown in Figure 10. This prediction agrees with the experimental observations to within 5%. The stress-strain shear curve at the center of the ligament is also shown in Figure 10. It can be seen that the average stress-strain shear curve *underestimates* the actual stresses. The difference, which is not large, is the result of the assumption that the shear stress and strain are almost uniform across the minimum section. The results of the finite element analysis shown in Figure 11 indicate that the shear stress at the minimum section is essentially constant therefore justifying the use of the Iosipescu specimen as a means of obtaining shear data. Lastly, the hypothesis made to write the evolution of the inelastic strain α_{12} (Eq. (31)) as a function of the equivalent shear stress τ_{eq} (Eq. (32)) seems reasonable when the results of prediction of the Iosipescu test is compared with the experiments. Figure 11 also compares the shear stress profile for the linear elastic and non-linear calculations when the external load level is identical. The effect of non-linear stress/strain behavior allows the stresses to be redistributed when compared to a purely linear elastic calculation. This effect can be measured by the ratio of the average to maximum shear stresses in the elastic calculation (0.93) and in the non-linear analysis

(0.95). This difference is not important since the shear stress profile is almost constant in the ligament even for a linear elastic computation.

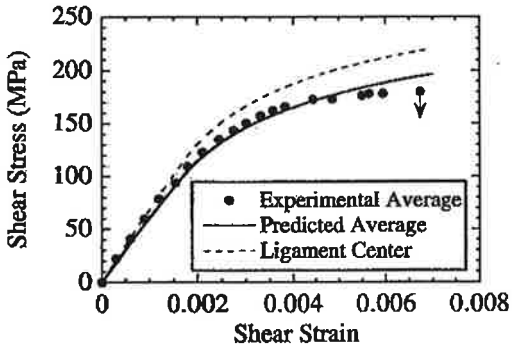

Fig. 10. – Experimental and predicted evolution of the average shear stresses σ_{xy} as a function of the shear strains γ_{xy} in a Iosipescu test on a [0/90] SiC/SiC lay-up. This evolution is compared with the evolution of the shear stresses σ_{xy} as a function of the shear strains γ_{xy} in the center of the specimen.

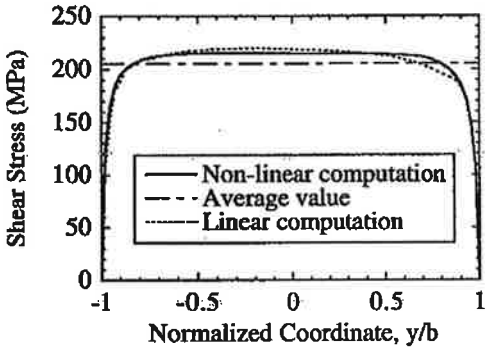

Fig. 11. – Shear stress profile in the ligament of the Iosipescu specimen when the shear strain γ_{xy} in the center of the specimen is equal to 0.007 as a function of the relative distance y/b from the center of the ligament for a linear and non-linear computation.

6. Conclusions

A CDM model is proposed for CMCs which is mechanisms-based. The laws which relate the growth of the internal state variables to their associated forces have been derived from the unloading-reloading paths during tensile experiments for two different directions. The ability of the model to predict the response to another state of stress suggests the advantage of a mechanisms-based approach.

When applied to SiC/SiC [0/90] lay-ups, the present model has ten internal variables, viz. three inelastic strains modeling sliding, three damage variables describing the amount of debonding and four damage variables accounting for matrix-cracking and fiber-breakage in the two plies. It is shown that only two different experiments in tension are needed to identify the growth laws of the ten internal variables. The

model has the potential to be applied to other material configurations (e.g., SiC/CAS, SiC/C, C/C, and presumably SiC/Al_2O_3 composites) and architectures (e.g., woven configurations). Furthermore, the general framework presented herein has been applied to room temperature configurations and monotonic loading conditions. However extensions to cyclic load histories as well as high temperature applications can be included with minimal change to the state potential formulations. Evolution laws will have to be modified slightly.

The reliability of the Iosipescu test is confirmed as a means of average stress-strain shear data, and the constitutive equations are able to predict the shear properties correctly. However, it is shown that the average shear properties may be slightly different from the actual stress-strain shear data in the center of the ligament. Therefore the identification of the shear properties based upon the measurements on a Iosipescu test are, strictly speaking, only an approximation of the actual response in pure shear.

The ability of stress redistribution due to the non-linearity of the stress/strain curve has been shown in the case of the Iosipescu experiment. Stress redistribution is important for structural applications and needs to be further studied on other types of structures and load configurations (e.g., plates with holes, notches, pin-loaded structures). This work is still under way.

Acknowledgments

This work was supported by the Advanced Research Project Agency through the University Research Initiative under Office of Naval Research Contract No. N-00014-92-J-1808.

APPENDIX

Let us consider a lamina with initial principal directions of orthotropy given by 1 and 2. The initial principal directions of orthotropy, or material directions, often do not coincide with the loading directions given by x and y (*Fig.* 5). The z-axis is perpendicular to the plan (1-2) and (x-y).

Under plane stress conditions, an elastic stress-strain relation in the material directions can be written in terms of the compliance matrix $\{S\}$.

$$\begin{pmatrix} \varepsilon_{11} \\ \varepsilon_{22} \\ \gamma_{12} \end{pmatrix} = \begin{pmatrix} S_{11} & S_{12} & 0 \\ S_{12} & S_{22} & 0 \\ 0 & 0 & S_{66} \end{pmatrix} \begin{pmatrix} \sigma_{11} \\ \sigma_{22} \\ \sigma_{12} \end{pmatrix} \tag{A1.1}$$

or in terms of the stiffness matrix $\{Q\}$

$$\begin{pmatrix} \sigma_{11} \\ \sigma_{22} \\ \sigma_{12} \end{pmatrix} = \begin{pmatrix} Q_{11} & Q_{12} & 0 \\ Q_{12} & Q_{22} & 0 \\ 0 & 0 & Q_{66} \end{pmatrix} \begin{pmatrix} \varepsilon_{11} \\ \varepsilon_{22} \\ \gamma_{12} \end{pmatrix} \tag{A1.2}$$

If we now consider the same expression written in the loading directions, the general stress-strain relation leads to a full compliance matrix $\{\overline{S}\}$

$$\text{(A2.1)} \qquad \begin{pmatrix} \varepsilon_{xx} \\ \varepsilon_{yy} \\ \gamma_{xy} \end{pmatrix} = \begin{pmatrix} \overline{S}_{11} & \overline{S}_{12} & \overline{S}_{16} \\ \overline{S}_{12} & \overline{S}_{22} & \overline{S}_{26} \\ \overline{S}_{16} & \overline{S}_{26} & \overline{S}_{66} \end{pmatrix} \begin{pmatrix} \sigma_{xx} \\ \sigma_{yy} \\ \sigma_{xy} \end{pmatrix}$$

or to a full compliance matrix $\{\overline{Q}\}$

$$\text{(A2.2)} \qquad \begin{pmatrix} \sigma_{xx} \\ \sigma_{yy} \\ \sigma_{xy} \end{pmatrix} = \begin{pmatrix} \overline{Q}_{11} & \overline{Q}_{12} & \overline{Q}_{16} \\ \overline{Q}_{12} & \overline{Q}_{22} & \overline{Q}_{26} \\ \overline{Q}_{16} & \overline{Q}_{26} & \overline{Q}_{66} \end{pmatrix} \begin{pmatrix} \varepsilon_{xx} \\ \varepsilon_{yy} \\ \gamma_{xy} \end{pmatrix}$$

The relationship between the compliance matrix in the material directions, $\{S\}$, and in the loading directions, $\{\overline{S}\}$ can be written as follows

$$\text{(A3.1)} \qquad \{\overline{S}\} = \{T\}^T \{S\} \{T\}$$

and the relationship between the stiffness matrix in the material directions, $\{Q\}$, and in the loading directions, $\{\overline{Q}\}$ can be written as follows

$$\text{(A3.2)} \qquad \{\overline{Q}\} = \{T\}^{-1} \{Q\} \{T\}^{-T}$$

where the superscript ^{T} denotes the matrix transpose, and $\{T\}$ the transformation matrix associated with a positive rotation of angle θ of principal axes about z from material axes (*Fig.* 1)

$$\text{(A4)} \qquad \{T\} = \begin{pmatrix} \cos^2\theta & \sin^2\theta & -2\sin\theta\cos\theta \\ \sin^2\theta & \cos^2\theta & 2\sin\theta\cos\theta \\ \sin\theta\cos\theta & -\sin\theta\cos\theta & \cos^2\theta - \sin^2\theta \end{pmatrix}$$

REFERENCES

ASHBY M. F., 1992, Physical Modeling of Materials Problems, *Mat. Sci. Tech.*, **8**, 102-111.

AVESTON J., COOPER G. A., KELLY A., 1971, *Single and Multiple Fracture, National Physical Laboratory: Properties of Fiber Composites*, IPC Science and Technology Press, Surrey (UK), 15-26.

BEYERLEY D., SPEARING S. M., ZOK F. W., EVANS A. G., 1992, Damage, Degradation and Failure in a Unidirectional Ceramic-Matrix Composite, *J. Am. Ceram. Soc.*, **75**, n° 10, 2719-2725.

BUDIANSKY B., O'CONNELL R. J., 1976, Elastic Moduli of a Cracked System, *Int. J. Solids Struct.*, **12**, 81-97.

BURR A., HILD F., LECKIE F. A., 1995, Micro-Mechanics and Continuum Damage Mechanics, *Arch. Appl. Mech.*, **65**, n° 7, 437-456.

CADY C., HEREDIA F. E., EVANS A. G., 1995*a*, In-Plane Mechanical Properties of Several Ceramic-Matrix Composites, *J. Am. Ceram. Soc.*, **78**, n° 8, 2065-2078.

CADY C., MAKIN T. J., EVANS A. G., 1995*b*, Silicon Carbide Calcium Aluminosilicate – A Notch-Insensitive Ceramic-Matrix Composite, *J. Am. Ceram. Soc.*, **78**, n° 1, 77-82.

CHABOCHE J. L., 1982, Le concept de contrainte effective appliqué à l'élasticité et à la viscoplasticité en présence d'un endommagement anisotrope, *Colloque international du CNRS*, **295**, 31-43.

COCKS A. C. F., LECKIE F. A., 1987, Creep Constitutive Equations for Damaged Materials, in *Advances in Applied Mechanics*, Academic Press, New York, **25**, 239-294.

COLEMAN D. B., GURTIN M. E., 1967, Thermodynamics with Internal Variables, *J. Chem. Phys.*, **47**, 597-613.

CURTIN W. A., 1991, Exact Theory of Fiber Fragmentation in Single-Filament Composite, *J. Mat. Sci.*, **26**, 5239-5253.

DRUCKER D. C., PRAGER W., 1956, Soil Mechanics and Plastic Analysis of Limit Design, *Quat. of Appl. Math.*, **14**.

ESHELBY J. D., 1957, The Determination of the Elastic Field of an Ellipsoidal Inclusion and Related Problems, *Proc. Roy. Soc. London*, **A241**, 376-396.

EVANS A. G., DOMERGUE J. M., VAGAGGINI E., 1994, Methodology for Relating the Tensile Constitutive Behavior of Ceramic matrix Composites to Constituent Properties, *J. Am. Ceram. Soc.*, **77**, n° 6, 1425-1435.

GERMAIN P., NGUYEN Q. S., SUQUET P., 1983, Continnum Thermodynamics, *J. Appl. Mech.*, **50**, 1010-1020.

HEREDIA F. E., EVANS A. G., ANDERSON C. A., 1995, Tensile and Shear Properties of Continuous Fiber-Reinforced SiC/Al_2O_3 Composites Processed by Melt Oxidation, *J. Am. Ceram. Soc.*, **78**, n° 10, 2790-2800.

HIBBITT H. D., KARLSSON B. I., SORENSEN P., 1995, *Abaqus, version 5.5.*

HILD F., BURR A., LECKIE F. A., 1996, Matrix-Cracking and Debonding in Ceramic-Matrix Composites, *Int. J. Solids Struct.*, **33**, n° 8, 1209-1220.

HUTCHINSON J. W., JENSEN H. M., 1990, Models for Fiber Debonding and Fiber Pull-Out in Brittle Composites with Friction, *Mech. Mat.*, **9**, 139-163.

IOSIPESCU N., 1967, New Accurate Procedure for Single Shear Testing of Metals, *J. Mater.*, **2**, 537-566.

JANSSON S., LECKIE F. A., 1993, The Mechanics of Failure of Silicon Carbide Fiber-Reinforced Glass-Matrix Composites, *Acta Metall. Mat.*, **40**, n° 11, 2967-2978.

LADEVÈZE P., 1983, *Sur une théorie de l'endommagement anisotrope*, LMT Cachan, Report N° 34.

LEMAITRE J., 1992, *A Course on Damage Mechanics*, Springer-Verlag, Berlin (Germany).

LEMAITRE J., CHABOCHE J.-L., 1978, Aspect phénoménologique de la rupture par endommagement, *J. Méc. Appl.*, **2**, n° 3, 317-365.

LOVE A. E. H., 1927, *The Mathematical Theory of Elasticity*, Cambridge University Press, Cambridge (UK).

PLUVINAGE P., 1991, *Étude expérimentale et simulation numérique du comportement mécanique de matériaux composites SiC/SiC, Influence des paramètres de stratification et d'élaboration*, Thèse d'Université, Bordeaux-I.

RICE J. R., 1971, Inelastic Constitutive Relations for Solids: An Internal Variable Theory and its Application to Metal Plasticity, *J. Mech. Phys. Solids*, **19**, 433-455.

VOLTERRA V., 1907, Sur l'équilibre des corps élastiques multiplement connexes, *Annales Scientifiques de l'École Normale Supérieure*, **24**, n° 3, 401-518.

WEIBULL W., 1939, A Statistical Theory of the Strength of Materials, *Roy. Swed. Inst. Eng. Res.*, **151**.

WEIBULL W., 1951, A Statistical Distribution Function of Wide Applicability, *J. Appl. Mech.*, **18**, n° 3, 293-297.

ZIENKIEVICZ O. C., TAYLOR R. L., 1989, *The Finite Element Method*, McGraw-Hill, London (UK), 4th edition.